

Seismic response of SiO₂ nanoparticles-reinforced concrete pipes based on DQ and newmark methods

Mohsen Motezaker¹ and Reza Kolahchi^{*2}

¹Department of Civil Engineering, School of Science and Engineering, Sharif University of Technology, International Campus, Kish Island, Iran

²Department of Civil Engineering, Meymeh Branch, Islamic Azad University, Meymeh, Iran

(Received April 11, 2017, Revised May 9, 2017, Accepted May 18, 2017)

Abstract. Dynamic analysis of a concrete pipes armed with Silica (SiO₂) nanoparticles subjected to earthquake load is presented. The structure is modeled with first order shear deformation theory (FSDT) of cylindrical shells. Mori-Tanaka approach is applied for obtaining the equivalent material properties of the structure considering agglomeration effects. Based on energy method and Hamilton's principle, the motion equations are derived. Utilizing the harmonic differential quadrature method (HDQM) and Newmark method, the dynamic displacement of the structure is calculated for the Kobe earthquake. The effects of different parameters such as geometrical parameters of pipe, boundary conditions, SiO₂ volume percent and agglomeration are shown on the dynamic response of the structure. The results indicate that reinforcing the concrete pipes by SiO₂ nanoparticles leads to a reduction in the displacement of the structure during an earthquake.

Keywords: seismic analysis; concrete pipes; SiO₂ nanoparticles; agglomeration; HDQM

1. Introduction

Concrete pipe has a rich history, spawning an industry that today produces an economical, high quality product for numerous applications. It's been in use for over 5,000 years. Concrete pipes have a proven track record and are custom designed for user applications including drainage, sewerage, water supply and irrigation. Nowadays, the application of nano materials has received numerous attentions to enhance the conventional concrete properties. Eventually, the introduction of nano materials in concrete is to increase its strength and durability. Nano material is defined as material that contains particle size which less than 200 nm.

There are many works in the concrete pipes in the literature. Seismic response of buried pipes in longitudinal direction was studied by Nedjar *et al.* (2007). The effect of the variation of geotechnical properties of the surrounding soil on the stiffness, mass and damping of the soil was considered. A comprehensive experimental and analytical study of pipe-pin hinges was completed by Zaghi and Saiidi (2010). Tests of large-scale models of the hinges were conducted and showed that lateral failure mechanism is typically controlled by concrete diagonal tensile cracking in combination with flexural hinging of the steel pipe as opposed to pure shear failure of the pipe. The temperature gradient properties of the concrete around a pipe were studied by Zhu *et al.* (2013). A new calculation method was developed based on these properties and an explicit iterative algorithm. Using a mesoscopic finite-element (FE) mesh,

three-phase composites of concrete namely aggregate, mortar matrix and interfacial transition zone (ITZ) were modeled by Zhang *et al.* (2015). An equivalent probabilistic model was presented for failure study of concrete by assuming that the material properties conform to the Weibull distribution law. Vibration and stability of concrete pipes reinforced with carbon nanotubes (CNTs) conveying fluid were presented by Zamani Nouri *et al.* (2016). Due to the existence of CNTs, the structure is subjected to magnetic field. Cheraghi and Zahrai (2016) presented a multi-level pipe in pipe passive control system and its cyclic behavior is evaluated with nonlinear static and dynamic analyses using finite element method by ABAQUS software. Then, hysteresis curves were studied representing a highly ductile behavior for the proposed damper. Mahjoubi and Maleki (2016) provided guidelines for implementing Dual-pipe damper (DPD) in actual steel buildings, evaluate and compare their performance against other metallic dampers. Failure analysis of a cracked concrete pipe in a 50 MW thermosolar power plant was investigated by González-Nicieza *et al.* (2017). Simulations show that failure was caused by additional overloads. Lai *et al.* (2017) developed and benchmarks detailed 3D finite element method (FEM) models for evaluating the seismic behavior of spirally welded pipes (SWP), Fully filled SWP, and partially filled SWP. The FEM models account for behavioral complexities such as steel yielding, pipe local buckling and fracture, concrete cracking and crushing, cyclic stiffness degradation and recovery, and effects of concrete confinement.

None of the above paper has been work on the mathematical modeling of the concrete structures. The nonlinear buckling of straight concrete columns armed with single-walled carbon nanotubes (SWCNTs) and SiO₂

*Corresponding author
E-mail: r.kolahchi@gmail.com

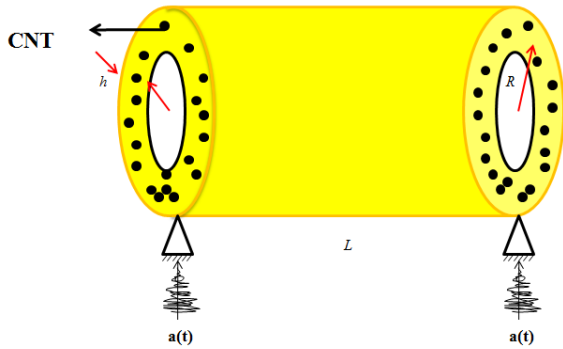


Fig. 1 A schematic figure of nanocomposite pipe covered by piezoelectric layer conveying fluid under seismic load

nanoparticles resting on foundation was investigated by Jafarian Arani *et al.* (2016) and Zamanian *et al.* (2016). the nonlinear buckling of straight concrete columns armed with single-walled carbon nanotubes (SWCNTs) resting on foundation was investigated by Safari Bilouei *et al.* (2016). Stress analysis of concrete pipes reinforced with Al_2O_3 nanoparticles was presented by Heidarzadeh *et al.* (2016) considering agglomeration effects.

To the best of author knowledge, no theoretical report has been found in the literature on seismic analysis of concrete pipes reinforced with SiO_2 nanoparticles. Motivated by these considerations, we aim to present a mathematical model for seismic analysis of concrete pipe reinforced with SiO_2 nanoparticles considering agglomeration effects based on Mori-Tanaka approach. Based on FSDT model, the motion equations are derived using energy method and Hamilton's principal. Using HDQM and Newmark method, the dynamic deflection of the structure is calculated and the effects of different parameters such as volume percent of SiO_2 nanoparticles, SiO_2 agglomeration, geometrical parameters and boundary conditions on the dynamic deflection of the structure are shown.

2. Formulation and modeling

As shown in Fig. 1, a concrete pipe reinforced with SiO_2 nanoparticles subjected to earthquake load is presented where the geometrical parameters of length L , radius R and thickness h are shown.

According to FSDT, the displacement field can be written as (Brush and Almoth 1975)

$$u(x, \theta, z, t) = u(x, \theta, t) + z\psi_x(x, \theta, t), \quad (1)$$

$$v(x, \theta, z, t) = v(x, \theta, t) + z\psi_\theta(x, \theta, t), \quad (2)$$

$$w(x, \theta, z, t) = w(x, \theta, t), \quad (3)$$

In which ψ_x and ψ_θ are the angle of rotation around the x and θ axes, respectively. By substituting Eqs. (1)-(3) into the strain-displacement relations, we have

$$\varepsilon_{xx} = \frac{\partial u}{\partial x} + z \frac{\partial \psi_x}{\partial x}, \quad (4)$$

$$\varepsilon_{\theta\theta} = \frac{\partial v}{R\partial\theta} + \frac{w}{R} + z \frac{\partial \psi_\theta}{R\partial\theta}, \quad (5)$$

$$\gamma_{x\theta} = \frac{\partial v}{\partial x} + \frac{\partial u}{R\partial\theta} + z \left(\frac{\partial \psi_x}{R\partial\theta} + \frac{\partial \psi_\theta}{\partial x} \right). \quad (6)$$

$$\gamma_{xz} = \frac{\partial w}{\partial x} + \psi_x, \quad (7)$$

$$\gamma_{\theta z} = \frac{\partial w}{R\partial\theta} - \frac{v}{R} + \psi_\theta. \quad (8)$$

According to Hook's law, the constitutive equation of the concrete pipe is expressed as follows

$$\begin{bmatrix} \sigma_{xx} \\ \sigma_{\theta\theta} \\ \tau_{\theta z} \\ \tau_{xz} \\ \tau_{x\theta} \end{bmatrix} = \begin{bmatrix} C_{11} & C_{12} & 0 & 0 & 0 \\ C_{12} & C_{22} & 0 & 0 & 0 \\ 0 & 0 & C_{44} & 0 & 0 \\ 0 & 0 & 0 & C_{55} & 0 \\ 0 & 0 & 0 & 0 & C_{66} \end{bmatrix} \begin{bmatrix} \varepsilon_{xx} \\ \varepsilon_{\theta\theta} \\ \gamma_{\theta z} \\ \gamma_{xz} \\ \gamma_{x\theta} \end{bmatrix}, \quad (8)$$

where the effective material properties of the concrete pipe reinforced with SiO_2 nanoparticles (C_{ij}) can be calculated based on Mori-Tanaka approach (Appendix A).

The strain energy of the structure is given by

$$U = \int_V \left[(\sigma_{xx}\varepsilon_{xx} + \sigma_{\theta\theta}\varepsilon_{\theta\theta} + \tau_{x\theta}\gamma_{x\theta} + \tau_{xz}\gamma_{xz} + \tau_{z\theta}\gamma_{z\theta}) \right] dV. \quad (10)$$

By substituting Eqs. (4)-(8) into Eq. (10) the strain energy can be expressed as follows

$$\begin{aligned} U = & \frac{1}{2} \int_z \int_0^{2\pi} \int_0^L \left\{ \sigma_{xx} \left[\frac{\partial u}{\partial x} + z \frac{\partial \psi_x}{\partial x} \right] + \sigma_{\theta\theta} \left[\frac{1}{R} \left(w + \frac{\partial v}{\partial \theta} \right) \right. \right. \\ & \left. \left. + \frac{z}{R} \frac{\partial \psi_\theta}{\partial \theta} \right] + \tau_{x\theta} \left(\frac{\partial v}{\partial x} + \frac{1}{R} \frac{\partial u}{\partial \theta} + z \frac{\partial \psi_\theta}{\partial x} + \frac{z}{R} \frac{\partial \psi_x}{\partial \theta} \right) \right. \\ & \left. + \tau_{z\theta} \left[\frac{1}{R} \left(\frac{\partial w}{\partial \theta} - v \right) + \psi_\theta \right] + (\tau_{xz}) \left(\psi_x + \frac{\partial w}{\partial x} \right) \right\} R dx d\theta dz, \end{aligned} \quad (11)$$

By introducing the stress resultants as below

$$\begin{Bmatrix} N_{xx} \\ N_{\theta\theta} \\ N_{x\theta} \end{Bmatrix} = \int_{-h}^h \begin{Bmatrix} \sigma_{xx} \\ \sigma_{\theta\theta} \\ \tau_{x\theta} \end{Bmatrix} dz, \quad (12)$$

$$\begin{Bmatrix} Q_x \\ Q_\theta \end{Bmatrix} = k' \int_{-h}^h \begin{Bmatrix} \sigma_{xz} \\ \tau_{\theta z} \end{Bmatrix} dz, \quad (13)$$

$$\begin{Bmatrix} M_{xx} \\ M_{\theta\theta} \\ M_{x\theta} \end{Bmatrix} = \int_{-h}^h \begin{Bmatrix} \sigma_{xx} \\ \sigma_{\theta\theta} \\ \tau_{x\theta} \end{Bmatrix} z dz, \quad (14)$$

we have

$$U = 0.5 \int \left(N_{xx} \frac{\partial u}{\partial x} + N_{\theta\theta} \left(\frac{\partial v}{R \partial \theta} + \frac{w}{R} \right) + Q_{\theta} \left(\frac{\partial w}{R \partial \theta} - \frac{v}{R} + \psi_{\theta} \right) + Q_x \left(\frac{\partial w}{\partial x} + \psi_x \right) + N_{x\theta} \left(\frac{\partial v}{\partial x} + \frac{\partial u}{R \partial \theta} \right) + M_{xx} \frac{\partial \psi_x}{\partial x} + M_{\theta\theta} \frac{\partial \psi_{\theta}}{R \partial \theta} + M_{x\theta} \left(\frac{\partial \psi_x}{R \partial \theta} + \frac{\partial \psi_{\theta}}{\partial x} \right) \right) dA, \quad (15)$$

where k' is the shear correction factor.

The kinetic energy of the structure is

$$U = \frac{\rho}{2} \int (\dot{u}^2 + \dot{v}^2 + \dot{w}^2) dV, \quad (16)$$

where ρ is the equivalent density of the nanocomposite pipe. Substituting Eqs. (1)-(3) into Eq. (16), we have

$$K = \frac{\rho}{2} \int \left(\left(\frac{\partial u}{\partial t} + z \frac{\partial \psi_x}{\partial t} \right)^2 + \left(\frac{\partial v}{\partial t} + z \frac{\partial \psi_{\theta}}{\partial t} \right)^2 + \left(\frac{\partial w}{\partial t} \right)^2 \right) dV. \quad (17)$$

By defining the following terms

$$\begin{Bmatrix} I_0 \\ I_1 \\ I_2 \end{Bmatrix} = \int_{-h}^h \begin{Bmatrix} \rho \\ \rho z \\ \rho z^2 \end{Bmatrix} dz, \quad (18)$$

Eq. (17) can be rewritten as below

$$K = 0.5 \int \left[I_0 \left(\left(\frac{\partial u}{\partial t} \right)^2 + \left(\frac{\partial v}{\partial t} \right)^2 + \left(\frac{\partial w}{\partial t} \right)^2 \right) + 2I_1 \left(\frac{\partial u}{\partial t} \frac{\partial \psi_x}{\partial t} + \frac{\partial v}{\partial t} \frac{\partial \psi_{\theta}}{\partial t} \right) + I_2 \left(\left(\frac{\partial \psi_x}{\partial t} \right)^2 + \left(\frac{\partial \psi_{\theta}}{\partial t} \right)^2 \right) \right] dA. \quad (19)$$

The external work due to the earthquake loads can be computed as below

$$W_s = \int \underbrace{(ma(t))}_{F_{Seismic}} w dA, \quad (20)$$

where m and $a(t)$ are the mass and the acceleration of the earth.

The motion equations of the structure are derived using the Hamilton's principle which is considered as follows

$$\int_0^t (\delta U - \delta K - \delta W) dt = 0. \quad (21)$$

Now, by applying the Hamilton's principle and after integration by part and some algebraic manipulation, five equations of motion can be derived as follows

$$\delta u : \frac{\partial N_{xx}}{\partial x} + \frac{\partial N_{x\theta}}{R \partial \theta} = I_0 \frac{\partial^2 u}{\partial t^2} + I_1 \frac{\partial^2 \psi_x}{\partial t^2}, \quad (22)$$

$$\delta v : \frac{\partial N_{x\theta}}{\partial x} + \frac{\partial N_{\theta\theta}}{R \partial \theta} + \frac{Q_{\theta}}{R} = I_0 \frac{\partial^2 v}{\partial t^2} + I_1 \frac{\partial^2 \psi_{\theta}}{\partial t^2}, \quad (23)$$

$$\delta w : \frac{\partial Q_x}{\partial x} + \frac{\partial Q_{\theta}}{R \partial \theta} + \frac{\partial}{\partial x} \left(N_x^f \frac{\partial w}{\partial x} \right) + \frac{\partial}{R \partial \theta} \left(N_{\theta}^f \frac{\partial w}{R \partial \theta} \right) + F_{Seismic} = I_0 \frac{\partial^2 w}{\partial t^2}, \quad (24)$$

$$\delta \psi_x : \frac{\partial M_{xx}}{\partial x} + \frac{\partial M_{x\theta}}{R \partial \theta} - Q_x = I_1 \frac{\partial^2 u}{\partial t^2} + I_2 \frac{\partial^2 \psi_x}{\partial t^2}, \quad (25)$$

$$\delta \psi_{\theta} : \frac{\partial M_{x\theta}}{\partial x} + \frac{\partial M_{\theta\theta}}{R \partial \theta} - Q_{\theta} = I_1 \frac{\partial^2 v}{\partial t^2} + I_2 \frac{\partial^2 \psi_{\theta}}{\partial t^2}. \quad (26)$$

By integrating the stress-strain relations of the structure using Eqs. (12)-(14) we have

$$N_{xx} = A_{11} \frac{\partial u}{\partial x} + B_{11} \left(\frac{\partial \psi_x}{\partial x} \right) + A_{12} + B_{12} \left(\frac{\partial \psi_{\theta}}{R \partial \theta} \right), \quad (27)$$

$$N_{\theta\theta} = A_{12} \frac{\partial u}{\partial x} + B_{12} \left(\frac{\partial \psi_x}{\partial x} \right) + A_{22} \left(\frac{\partial v}{R \partial \theta} + \frac{w}{R} \right) + B_{22} \left(\frac{\partial \psi_{\theta}}{R \partial \theta} \right), \quad (28)$$

$$N_{x\theta} = A_{66} \left(\frac{\partial u}{R \partial \theta} + \frac{\partial v}{\partial x} \right) + B_{66} \left(\frac{\partial \psi_x}{R \partial \theta} + \frac{\partial \psi_{\theta}}{\partial x} \right), \quad (29)$$

$$Q_x = A_{55} \left(\frac{\partial w}{\partial x} + \psi_x \right), \quad (30)$$

$$Q_{\theta} = A_{44} \left(\frac{\partial w}{R \partial \theta} - \frac{v}{R} + \psi_{\theta} \right), \quad (31)$$

$$M_{xx} = B_{11} \frac{\partial u}{\partial x} + D_{11} \left(\frac{\partial \psi_x}{\partial x} \right) + B_{12} \left(\frac{\partial v}{R \partial \theta} + \frac{w}{R} \right) + D_{12} \left(\frac{\partial \psi_{\theta}}{R \partial \theta} \right), \quad (32)$$

$$M_{\theta\theta} = B_{12} \frac{\partial u}{\partial x} + D_{12} \left(\frac{\partial \psi_x}{\partial x} \right) + B_{22} \left(\frac{\partial v}{R \partial \theta} + \frac{w}{R} \right) + D_{22} \left(\frac{\partial \psi_{\theta}}{R \partial \theta} \right), \quad (33)$$

$$M_{x\theta} = B_{66} \left(\frac{\partial u}{R \partial \theta} + \frac{\partial v}{\partial x} \right) + D_{66} \left(\frac{\partial \psi_x}{R \partial \theta} + \frac{\partial \psi_{\theta}}{\partial x} \right), \quad (34)$$

where the constants A_{ij} , B_{ij} , D_{ij} , E_{ij} and F_{ij} are equal to

$$(A_{11}, A_{12}, A_{22}, A_{44}, A_{55}, A_{66}) = \int_{-h/2}^{h/2} (C_{11}, C_{12}, C_{22}, C_{44}, C_{55}, C_{66}) dz \quad (35)$$

$$(B_{11}, B_{12}, B_{22}, B_{66}) = \int_{-h/2}^{h/2} (C_{11}, C_{12}, C_{22}, C_{66}) z dz, \quad (36)$$

$$(D_{11}, D_{12}, D_{22}, D_{66}) = \int_{-h/2}^{h/2} (C_{11}, C_{12}, C_{22}, C_{66}) z^2 dz. \quad (37)$$

Now, by substituting Eqs. (27)-(34) into the equations of motion Eqs. (22)-(26) we have

$$\begin{aligned}
& A_{11} \frac{\partial^2 u}{\partial x^2} + B_{11} \left(\frac{\partial^2 \psi_x}{\partial x^2} \right) + A_{12} \left(\frac{\partial^2 v}{R \partial x \partial \theta} + \frac{\partial w}{R \partial x} \right) \\
& + B_{12} \left(\frac{\partial^2 \psi_\theta}{R^2 \partial x \partial \theta} \right) + \frac{A_{66}}{R} \left(\frac{\partial^2 u}{R \partial \theta^2} + \frac{\partial^2 v}{\partial x \partial \theta} \right) \\
& + \frac{B_{66}}{R} \left(\frac{\partial^2 \psi_x}{R \partial \theta^2} + \frac{\partial^2 \psi_\theta}{\partial x \partial \theta} \right) = I_0 \frac{\partial^2 u}{\partial t^2} + I_1 \frac{\partial^2 \psi_x}{\partial t^2},
\end{aligned} \quad (38)$$

$$\begin{aligned}
& A_{66} \left(\frac{\partial^2 u}{R \partial \theta \partial x} + \frac{\partial^2 v}{\partial x^2} \right) + B_{66} \left(\frac{\partial^2 \psi_x}{R \partial \theta \partial x} + \frac{\partial^2 \psi_\theta}{\partial x^2} \right) \\
& + \frac{A_{12}}{R} \frac{\partial^2 u}{\partial x \partial \theta} + \frac{B_{12}}{R} \left(\frac{\partial^2 \psi_x}{\partial x \partial \theta} \right) + \frac{A_{22}}{R} \left(\frac{\partial^2 v}{R \partial \theta^2} + \frac{\partial w}{R \partial \theta} \right) \\
& + \frac{B_{22}}{R} \left(\frac{\partial^2 \psi_\theta}{R^2 \partial \theta^2} \right) = I_0 \frac{\partial^2 v}{\partial t^2} + I_1 \frac{\partial^2 \psi_\theta}{\partial t^2},
\end{aligned} \quad (39)$$

$$\begin{aligned}
& A_{55} \left(\frac{\partial^2 w}{\partial x^2} + \frac{\partial \psi_x}{\partial x} \right) - E_{15} \frac{\partial^2 \varphi}{\partial x^2} \\
& + \frac{A_{44}}{R} \left(\frac{\partial^2 w}{R \partial \theta^2} - \frac{\partial v}{R \partial \theta} + \frac{\partial \psi_\theta}{\partial \theta} \right) + \frac{\partial}{R \partial \theta} \left(N_\theta^f \frac{\partial w}{R \partial \theta} \right) \\
& + \frac{\partial}{\partial x} \left(N_x^f \frac{\partial w}{\partial x} \right) + F_{Seismic} = I_0 \frac{\partial^2 w}{\partial t^2},
\end{aligned} \quad (40)$$

$$\begin{aligned}
& B_{11} \frac{\partial^2 u}{\partial x^2} + D_{11} \left(\frac{\partial^2 \psi_x}{\partial x^2} \right) + B_{12} \left(\frac{\partial^2 v}{R \partial \theta \partial x} + \frac{\partial w}{R \partial x} + \frac{\partial^2 w}{R \partial \theta \partial x} \right) \\
& + D_{12} \left(\frac{\partial^2 \psi_\theta}{R \partial \theta \partial x} \right) + \frac{B_{66}}{R} \left(\frac{\partial^2 u}{R \partial \theta^2} + \frac{\partial^2 v}{\partial x \partial \theta} \right) - A_{55} \left(\frac{\partial w}{\partial x} + \psi_x \right) \\
& + \frac{D_{66}}{R} \left(\frac{\partial^2 \psi_x}{R \partial \theta^2} + \frac{\partial^2 \psi_\theta}{\partial x \partial \theta} \right) = I_1 \frac{\partial^2 u}{\partial t^2} + I_2 \frac{\partial^2 \psi_x}{\partial t^2},
\end{aligned} \quad (41)$$

$$\begin{aligned}
& B_{66} \left(\frac{\partial^2 u}{R \partial \theta \partial x} + \frac{\partial^2 v}{\partial x^2} \right) + D_{66} \left(\frac{\partial^2 \psi_x}{R \partial \theta \partial x} + \frac{\partial^2 \psi_\theta}{\partial x^2} \right) \\
& + \frac{B_{12}}{R} \frac{\partial^2 u}{\partial x \partial \theta} + \frac{D_{12}}{R} \left(\frac{\partial^2 \psi_x}{\partial x \partial \theta} \right) + \frac{B_{22}}{R} \left(\frac{\partial^2 v}{R \partial \theta^2} + \frac{\partial w}{R \partial \theta} \right) \\
& + \frac{D_{22}}{R} \left(\frac{\partial^2 \psi_\theta}{R \partial \theta^2} \right) - A_{44} \left(\frac{\partial w}{R \partial \theta} - \frac{v}{R} + \psi_\theta \right) = I_1 \frac{\partial^2 v}{\partial t^2} + I_2 \frac{\partial^2 \psi_\theta}{\partial t^2}.
\end{aligned} \quad (42)$$

Also, the boundary conditions are considered as below

- Clamped-Clamped supported

$$x = 0, L \Rightarrow u = v = w = \psi_x = \psi_\theta = 0, \quad (43)$$

- Simply-Simply supported

$$x = 0, L \Rightarrow u = v = w = \psi_\theta = M_{xx} = 0, \quad (44)$$

- Clamped-Simply supported

$$\begin{aligned}
x = 0 & \Rightarrow u = v = w = \psi_x = \psi_\theta = 0, \\
x = L & \Rightarrow u = v = w = \psi_x = M_{xx} = 0.
\end{aligned} \quad (45)$$

3. HDQM

HDQM is one of the numerical methods in which the governing differential equations turn into a set of first order algebraic equations by applying the weighting coefficients. In these methods, the one-dimensional and two-dimensional derivative of the function may be defined as follows (Kolahchi *et al.* 2015, 2016a, b)

$$\frac{d^n f_x(x_i, \theta_j)}{dx^n} = \sum_{k=1}^{N_x} A_{ik}^{(n)} f(x_k, \theta_j) \quad n = 1, \dots, N_x - 1. \quad (46)$$

$$\frac{d^m f_y(x_i, \theta_j)}{d\theta^m} = \sum_{l=1}^{N_\theta} B_{jl}^{(m)} f(x_i, \theta_l) \quad m = 1, \dots, N_\theta - 1. \quad (47)$$

$$\frac{d^{n+m} f_{xy}(x_i, \theta_j)}{dx^n d\theta^m} = \sum_{k=1}^{N_x} \sum_{l=1}^{N_\theta} A_{ik}^{(n)} B_{jl}^{(m)} f(x_k, \theta_l). \quad (48)$$

For choosing sampling grid points, the Chebyshev polynomials are used as follows

$$X_i = \frac{L}{2} \left[1 - \cos \left(\frac{i-1}{N_x-1} \pi \right) \right], \quad i = 1, \dots, N_x \quad (49)$$

$$\theta_i = \frac{2\pi}{2} \left[1 - \cos \left(\frac{i-1}{N_\theta-1} \pi \right) \right]. \quad i = 1, \dots, N_\theta \quad (50)$$

The weighting coefficients can be obtained by the following simple algebraic relations

$$A_{ij}^{(1)} = \begin{cases} \frac{(\pi/2)M(x_i)}{M(x_j)\sin[(x_i-x_j)/2\pi]} & \text{for } i \neq j, \quad i, j = 1, 2, \dots, N_x, \\ -\sum_{\substack{j=1 \\ j \neq i}}^{N_x} A_{ij}^{(1)} & \text{for } i = j, \quad i, j = 1, 2, \dots, N_x \end{cases} \quad (51)$$

$$B_{ij}^{(1)} = \begin{cases} \frac{(\pi/2)P(\theta_i)}{P(\theta_j)\sin[(\theta_i-\theta_j)\pi]} & \text{for } i \neq j, \quad i, j = 1, 2, \dots, N_\theta, \\ -\sum_{\substack{j=1 \\ j \neq i}}^{N_\theta} B_{ij}^{(1)} & \text{for } i = j, \quad i, j = 1, 2, \dots, N_\theta \end{cases} \quad (52)$$

in which

$$M(x_i) = \prod_{\substack{j=1 \\ j \neq i}}^{N_x} \sin \left(\frac{(x_i - x_j)\pi}{2} \right), \quad (53)$$

$$P(\theta_i) = \prod_{\substack{j=1 \\ j \neq i}}^{N_\theta} \sin \left(\frac{(\theta_i - \theta_j)\pi}{2} \right), \quad (54)$$

and for higher-order derivatives we have

$$A_{ij}^{(n)} = n \left(A_{ii}^{(n-1)} A_{ij}^{(1)} - \pi \text{ctg} \left(\frac{x_i - x_j}{2} \right) \pi \right), \quad (55)$$

$$B_{ij}^{(m)} = m \left(B_{ii}^{(m-1)} B_{ij}^{(1)} - \pi \text{ctg} \left(\frac{\theta_i - \theta_j}{2} \right) \pi \right). \quad (56)$$

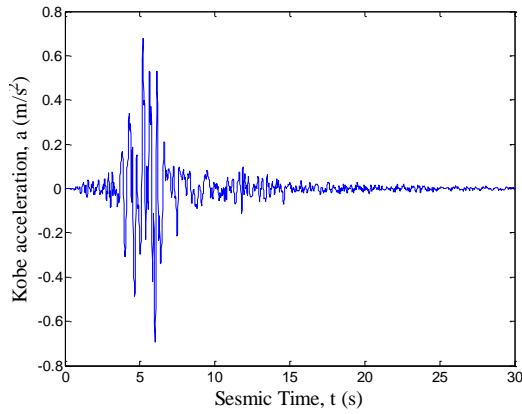


Fig. 2 Acceleration history of bam earthquake

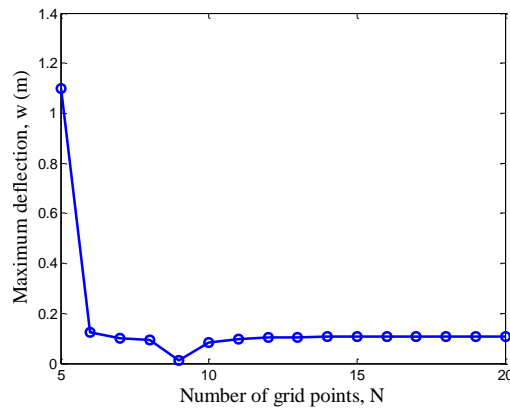


Fig. 3 Convergence and accuracy of HDQM

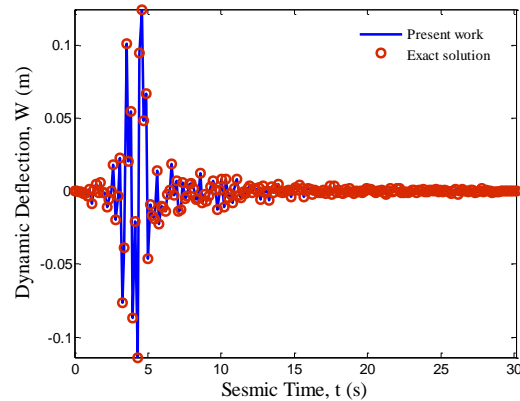


Fig. 4 Comparison of analytical and numerical results

Based on HDQM, the motion equations can be written in matrix form

$$\left([K] \begin{Bmatrix} \{d_b\} \\ \{d_d\} \end{Bmatrix} + [M] \begin{Bmatrix} \{\ddot{d}_b\} \\ \{\ddot{d}_d\} \end{Bmatrix} \right) = \begin{Bmatrix} \{0\} \\ \{-Ma(t)\} \end{Bmatrix}, \quad (57)$$

where $[K]$ and $[M]$ denote the stiffness matrix and the mass matrix, respectively. Also, $\{d_b\}$ and $\{d_d\}$ represent boundary and domain points, respectively.

4. Newmark method

In this section, Newmark method (Simsek 2010) is applied in the time domain to obtain the time response of the structure under the earthquake loads. Based on this method, Eq. (57) can be written in the general form as below

$$K^*(d_{i+1}) = Q_{i+1}, \quad (58)$$

where subscript $i+1$ indicates the time $t=t_{i+1}$, $K^*(d_{i+1})$ and Q_{i+1} are the effective stiffness matrix and the effective load vector which can be considered as

$$K^*(d_{i+1}) = K_L + K_{NL}(d_{i+1}) + \alpha_0 M + \alpha_1 C, \quad (59)$$

$$Q_{i+1}^* = Q_{i+1} + M \left(\alpha_0 \ddot{d}_i + \alpha_2 \dot{d}_i + \alpha_3 \ddot{d}_i \right) + C \left(\alpha_1 \dot{d}_i + \alpha_4 \ddot{d}_i + \alpha_5 \ddot{d}_i \right), \quad (60)$$

where (Simsek 2010)

$$\begin{aligned} \alpha_0 &= \frac{1}{\chi \Delta t^2}, & \alpha_1 &= \frac{\gamma}{\chi \Delta t}, & \alpha_2 &= \frac{1}{\chi \Delta t}, \\ \alpha_3 &= \frac{1}{2\chi} - 1, & \alpha_4 &= \frac{\gamma}{\chi} - 1, & \alpha_5 &= \frac{\Delta t}{2} \left(\frac{\gamma}{\chi} - 2 \right), \\ \alpha_6 &= \Delta t (1 - \gamma), & \alpha_7 &= \Delta t \gamma, \end{aligned} \quad (61)$$

in which $\gamma=0.5$ and $\chi=0.25$. Based on the iteration method, Eq. (58) is solved at any time step and modified velocity and acceleration vectors are calculated as follows

$$\ddot{d}_{i+1} = \alpha_0 (d_{i+1} - d_i) - \alpha_2 \dot{d}_i - \alpha_3 \ddot{d}_i, \quad (62)$$

$$\dot{d}_{i+1} = \dot{d}_i + \alpha_6 \ddot{d}_i + \alpha_7 \ddot{d}_{i+1}. \quad (63)$$

Then for the next time step, the modified velocity and acceleration vectors in Eqs. (62) and (63) are employed and all these procedures mentioned above are repeated.

5. Numerical results and discussion

In this section, the numerical results for the dynamic response of the concrete pipe which is reinforced by SiO₂ nanoparticles under the earthquake loads are examined. For this purpose, a concrete pipe of length to radius ratio of $L/R=10$ and thickness to radius ratio of $h/R=0.1$ is considered. The Yong modulus and Poison's ratio of concrete are $E_m=20 \text{ GPa}$ and $\nu_m=0.3$, respectively which is reinforced with agglomerated SiO₂ nanoparticles with Yong modulus of $E_r=75 \text{ GPa}$ and Poison's ratio of $\nu_r=0.3$. The case study of this paper is Kobe with the acceleration shown in Fig. 2.

Before, presenting the results of this work, studying the convergence of HDQM and validation of present model are two important issues. For convergence and accuracy of HDQM, Fig. 3 is plotted where the maximum dynamic deflection is changed with grid point numbers of HDQM. As shown, the maximum dynamic deflection decreases with increasing grid point numbers until in $N=17$, the results become converge. However, in this work, the grid point numbers for accurate results is chosen $N=17$. Fig. 4

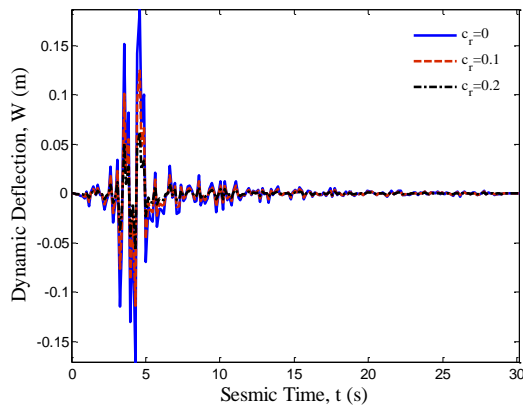


Fig. 5 The effect of SiO₂ nanoparticles volume percent on the dynamic deflection of the structure

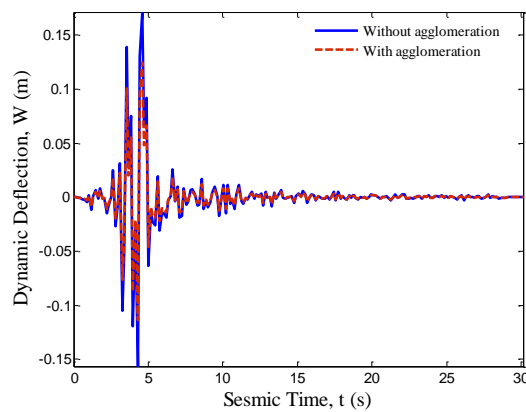


Fig. 6 The effect of SiO₂ nanoparticles agglomeration on the dynamic deflection of the structure

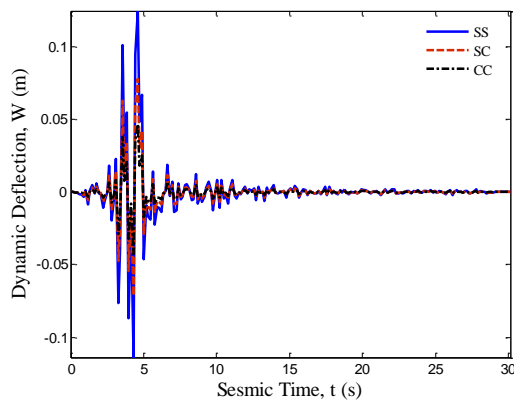


Fig. 7 The effect of boundary conditions on the dynamic deflection of the structure

illustrates the comparison of present results obtained by HDQM with the exact solution of this work for simply supported boundary conditions. It can be seen that the present results are in good agreement with exact solution, indicating validation of this work.

Figs. 5 and 6 show the effects of SiO₂ nanoparticles volume fraction and agglomeration of them on the maximum dynamic deflection of the structure. It can be found that with increasing the SiO₂ nanoparticles volume fraction, the maximum dynamic deflection decreases due to increase in the stiffness of the structure. In addition,

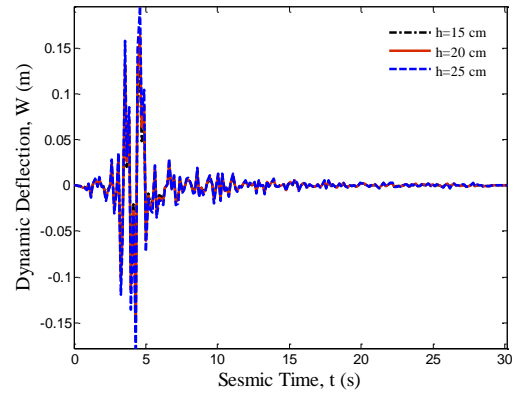


Fig. 8 The effect of pipe thickness on the dynamic deflection of the structure

according to Fig. 6, it is shown that considering agglomeration of SiO₂ nanoparticles leads to increase in the maximum dynamic deflection of the concrete structure. It is due to the fact that considering agglomeration effects leads to lower rigidity of system.

The effects of different boundary conditions on the maximum dynamic deflection are demonstrated in Fig. 7. Here, three types of boundary conditions are assumed as SS, CS and CC. As can be seen, the concrete pipe with CC boundary condition has lower maximum dynamic deflection with respect to other considered boundary conditions. It is because the concrete pipe with CC boundary condition has higher stiffness with respect to other considered boundary conditions.

Fig. 8 shows the effect of concrete pipe thickness on the maximum dynamic deflection. It is obvious that as the concrete pipe thickness increases, the maximum dynamic deflection of the structure decreases. It is due to the fact that increasing the concrete pipe thickness makes the structure stiffer.

6. Conclusions

Seismic response of the concrete pipes reinforced with SiO₂ nanoparticles based on a theoretical approach was the main contribution of this study. The concrete pipe was modeled with FSDT and the corresponding motion equations were derived by energy method and Hamilton's principle. The Mori-Tanaka model was for estimating the equivalent material properties of composite structure considering agglomeration effects. HDQM and Newmark methods were used for solution and calculating the dynamic deflection of the structure. The effects of different parameters such as thickness of pipe, boundary conditions, SiO₂ nanoparticles volume fraction and agglomeration were shown in the dynamic deflection of the structure. The results show that with increasing the SiO₂ nanoparticles volume fraction, the maximum dynamic deflection decreases. In addition, considering agglomeration of SiO₂ nanoparticles leads to increase in the maximum dynamic deflection of the concrete structure. Furthermore, the concrete pipe with CC boundary condition has lower maximum dynamic deflection with respect to other

considered boundary conditions. It was obvious that as the concrete pipe thickness increases, the maximum dynamic deflection.

485-501.

Zhu, Z., Qiang, S. and Chen, W. (2013), "A new method solving the temperature field of concrete around cooling pipes", *Comput. Concrete*, **11**(5), 441-462.

References

- Brush, D.O. and Almroth, B.O. (1975), *Buckling of Bars, Plates and Shells*, McGraw-Hill, New York, U.S.A.
- Cheraghi, A. and Zahrai, S.M. (2015), "Innovative multi-level control with concentric pipes along brace to reduce seismic response of steel frames", *J. Constr. Steel Res.*, **127**, 120-135.
- González-Nicieza, C., Ordiales-Martínez, V., Laín-Huerta, R., Laín-Huerta, C. and Álvarez-Fernández, M.I. (2017), "Failure analysis of a cracked concrete pipe in a 50 MW thermosolar power plant", *Eng. Fail. Anal.*, In press.
- Heidarzadeh, A., Kolahchi, R. and Rabani Bidgoli, M. (2016), "Concrete pipes reinforced with AL₂O₃ nanoparticles considering agglomeration: Magneto-thermo-mechanical stress analysis", *J. Civil Eng.*, 1-8.
- Jafarian Arani, A. and Kolahchi, R. (2016), "Buckling analysis of embedded concrete columns armed with carbon nanotubes", *Comput. Concrete*, **17**(5), 567-578.
- Kolahchi, R. and Moniribidgoli, A.M. (2016b), "Size-dependent sinusoidal beam model for dynamic instability of single-walled carbon nanotubes", *Appl. Math. Mech.*, **37**(2), 265-274.
- Kolahchi, R., Rabani Bidgoli, M., Beygipoor, G. and Fakhar, M.H. (2015), "A nonlocal nonlinear analysis for buckling in embedded FG-SWCNT-reinforced microplates subjected to magnetic field", *J. Mech. Sci. Technol.*, **29**(9), 3669-3677.
- Kolahchi, R., Safari, M. and Esmailpour, M. (2016a), "Dynamic stability analysis of temperature-dependent functionally graded CNT-reinforced visco-plates resting on orthotropic elastomeric medium", *Compos. Struct.*, **150**, 255-265.
- Lai, Z. and Varma, A.H. (2017), "Seismic behavior and modeling of concrete partially filled spirally welded pipes (CPF-SWP)", *Thin Wall Struct.*, **113**, 240-252.
- Mahjoubi, S. and Maleki, S. (2016), "Seismic performance evaluation and design of steel structures equipped with dual-pipe dampers", *J. Constr. Steel Res.*, **122**, 25-39.
- Nedjar, D., Hamane, M., Bensafi, M., Elachachi, S.M. and Breyse, D. (2007), "Seismic response analysis of pipes by a probabilistic approach", *Soil Dyn. Earthq. Eng.*, **27**(2), 111-115.
- Shi, D.L. and Feng, X. (2004), "The effect of nanotube waviness and agglomeration on the elastic property of carbon nanotube-reinforced composites", *J. Eng. Mater. Technol.*, **126**(3), 250-270.
- Simsek, M. (2010), "Non-linear vibration analysis of a functionally graded Timoshenko beam under action of a moving harmonic load", *Compos. Struct.*, **92**(10), 2532-2546.
- Simsek, M. (2010), "Non-linear vibration analysis of a functionally graded Timoshenko beam under action of a moving harmonic load", *Compos. Struct.*, **92**(10), 2532-2546.
- Zaghi, A.E. and Saiidi, M.S. (2010), "Seismic performance of pipe-pin two-way hinges in concrete bridge columns", *J. Earthq. Eng.*, **14**(8), 1253-1302.
- Zamani Nouri, A. (2017), "Mathematical modeling of concrete pipes reinforced with CNTs conveying fluid for vibration and stability analyses", *Comput. Concrete*, **19**(3), 325-331.
- Zamaniah, M., Kolahchi, R. and Rabani Bidgoli, M. (2016), "Agglomeration effects on the buckling behaviour of embedded concrete columns reinforced with SiO₂ nano-particles", *Wind Struct.*, **24**(1), 43-57.
- Zhang, C., Zhou, W., Ma, G., Hu, C. and Li, S. (2015), "A meso-scale approach to modeling thermal cracking of concrete induced by water-cooling pipes", *Comput. Concrete*, **15**(4),

CC

Appendix A

In this section, the Mori-Tanaka model is developed to examine the elastic properties of the SiO₂ nanoparticles-reinforced polymeric composite considering agglomeration effects (Shi and Feng 2004). The experimental results reveal that the most of SiO₂ nanoparticles dispersion irregularly and centralize in spherical shapes in the matrix (Shi and Feng 2004). These regions are called “inclusions” which have different elastic properties from the matrix material. V_r is the total volume of CNTs which given as below

$$V_r = V_r^{inclusion} + V_r^m \quad (A1)$$

in which $V_r^{inclusion}$ and V_r^m are the volumes of SiO₂ nanoparticles distributed in the spherical inclusions and in the matrix (concrete), respectively. Two following parameters are used to indicate the effect of agglomeration in the micromechanical model.

$$\xi = \frac{V_r^{inclusion}}{V}, \quad (A2)$$

$$\zeta = \frac{V_r^{inclusion}}{V_r}. \quad (A3)$$

C_r is the average volume fraction of SiO₂ nanoparticles in composite which is defined as follows

$$C_r = \frac{V_r}{V}. \quad (A4)$$

The volume fraction of the SiO₂ nanoparticles in the inclusions and in the matrix (concrete) can be related to each other as follows

$$\frac{V_r^{inclusion}}{V_{inclusion}} = \frac{C_r \zeta}{\xi}, \quad (A5)$$

$$\frac{V_r^m}{V - V_{inclusion}} = \frac{C_r (1 - \zeta)}{1 - \xi}. \quad (A6)$$

Assuming that the nanotubes are transversely isotropic and are distributed in the inclusions randomly, the inclusions are considered to be isotropic. Thereby, by applying Eshelby-Mori-Tanaka approach, the effective bulk modulus K and the effective shear modulus G of the isotropic materials can be written as below

$$K = K_{out} \left[1 + \frac{\xi \left(\frac{K_{in}}{K_{out}} - 1 \right)}{1 + \alpha (1 - \xi) \left(\frac{K_{in}}{K_{out}} - 1 \right)} \right], \quad (A7)$$

$$G = G_{out} \left[1 + \frac{\xi \left(\frac{G_{in}}{G_{out}} - 1 \right)}{1 + \beta (1 - \xi) \left(\frac{G_{in}}{G_{out}} - 1 \right)} \right], \quad (A8)$$

where K_{in} and K_{out} are the effective bulk modulus of the inclusion and the matrix outside the inclusion, respectively. Also, G_{in} and G_{out} are the effective shear modulus of the inclusion and the matrix outside the inclusion, respectively and are considered as follows

$$K_{in} = K_m + \frac{(\delta_r - 3K_m \chi_r) C_r \zeta}{3(\xi - C_r \zeta + C_r \zeta \chi_r)}, \quad (A9)$$

$$K_{out} = K_m + \frac{C_r (\delta_r - 3K_m \chi_r) (1 - \zeta)}{3[1 - \xi - C_r (1 - \zeta) + C_r \chi_r (1 - \zeta)]}, \quad (A10)$$

$$G_{in} = G_m + \frac{(\eta_r - 3G_m \beta_r) C_r \zeta}{2(\xi - C_r \zeta + C_r \zeta \beta_r)}, \quad (A11)$$

$$G_{out} = G_m + \frac{C_r (\eta_r - 3G_m \beta_r) (1 - \zeta)}{2[1 - \xi - C_r (1 - \zeta) + C_r \beta_r (1 - \zeta)]}, \quad (A12)$$

in which χ , β , δ and η can be calculated as

$$\chi_r = \frac{3(K_m + G_m) + k_r - l_r}{3(k_r + G_m)}, \quad (A13)$$

$$\beta_r = \frac{1}{5} \left\{ \frac{4G_m + 2k_r + l_r + \frac{4G_m}{3(k_r + G_m)} + \frac{4G_m}{(p_r + G_m)}}{2 \left[\frac{G_m (3K_m + G_m) + G_m (3K_m + 7G_m)}{G_m (3K_m + G_m) + m_r (3K_m + 7G_m)} \right]} \right\}, \quad (A14)$$

$$\delta_r = \frac{1}{3} \left[n_r + 2l_r + \frac{(2k_r - l_r)(3K_m + 2G_m - l_r)}{k_r + G_m} \right], \quad (A15)$$

$$\eta_r = \frac{1}{5} \left[\frac{2(n_r - l_r) + \frac{4G_m p_r}{(p_r + G_m)} + \frac{2(k_r - l_r)(2G_m + l_r)}{3(k_r + G_m)}}{\frac{8G_m m_r (3K_m + 4G_m)}{3K_m (m_r + G_m) + G_m (7m_r + G_m)}} \right].$$

Also, K_m and G_m are the bulk and shear modulus of the matrix phase which are given as below

$$K_m = \frac{E_m}{3(1 - 2\nu_m)}, \quad (A16)$$

$$G_m = \frac{E_m}{2(1 + \nu_m)}. \quad (A17)$$

Furthermore, α and β which mentioned in Eqs. (A7) and (A8) are defined as follows

$$\alpha = \frac{(1 + \nu_{out})}{3(1 - \nu_{out})}, \quad (A18)$$

$$\beta = \frac{(1 + \nu_{out})}{3(1 - \nu_{out})}, \quad (A19)$$

$$\nu_{out} = \frac{3K_{out} - 2G_{out}}{6K_{out} + 2G_{out}}. \quad (A20)$$

Eventually, the effective Young's modulus E and Poisson's ratio ν of the composite are given by

$$E = \frac{9KG}{3K + G} \quad , \quad (\text{A21})$$

$$\nu = \frac{3K - 2G}{6K + 2G} \quad . \quad (\text{A22})$$

So with obtaining E and ν , stiffness matrix of the structure can be calculated.